Vol. 148: 127–144, 2022
https://doi.org/10.3354/dao03648

DISEASES OF AQUATIC ORGANISMS
Dis Aquat Org

Published online March 31

Keeping up with advances in qPCR pathogen detection: an example for QPX disease in hard clams

Sabrina Geraci-Yee, Bassem Allam*, Jackie L. Collier

School of Marine and Atmospheric Sciences, Stony Brook University, Stony Brook, New York 11794-5000, USA

ABSTRACT: With marine diseases on the rise and increased reliance on molecular tools for disease surveillance, validated pathogen detection capabilities are important for effective management, mitigation, and response to disease outbreaks. At the same time, in an era of continual evolution and advancement of molecular tools for pathogen detection, it is critical to regularly reassess previously established assays to incorporate improvements of common practices and procedures, such as the minimum information for publication of quantitative real-time PCR experiments (MIQE) guidelines. Here, we reassessed, re-optimized, and improved the quantitative PCR (qPCR) assay routinely used for Quahog Parasite Unknown (QPX) disease monitoring. We made 19 significant changes to the qPCR assay, including improvements to PCR amplification efficiency, DNA extraction efficiency, inhibition testing, incorporation of linearized standards for absolute quantification, an inter-plate calibration technique, and improved conversion from copy number to number of cells. These changes made the assay a more effective and efficient tool for disease monitoring and pathogen detection, with an improved linear relationship with histopathology compared to the previous version of the assay. To support the wide adoption of validated qPCR assays for marine pathogens, we provide a simple workflow that can be applied to the development of new assays, re-optimization of old or suboptimal assays, or assay validation after changes to the protocol and a MIQE-compliant checklist that should accompany any published qPCR diagnostic assay to increase experimental transparency and reproducibility amongst laboratories.

KEY WORDS: Quantitative PCR · qPCR · Quahog Parasite Unknown · QPX · *Mucochytrium quahogii* · *Mercenaria mercenaria* · MIQE · Diagnostic assays · Pathology · Absolute quantification

1. INTRODUCTION

Over the past 3 decades, there has been an increase in epizootics of infectious diseases in marine systems including increasing reports of diseases in mollusks (Harvell et al. 2004, Lafferty et al. 2004, Ward & Lafferty 2004, Burge et al. 2013). Disease management practices suitable for most marine organisms are limited to reducing pathogen impact and inputs, which requires extensive knowledge on pathogen biology and ecology (Harvell et al. 2004, McCallum et al. 2004, Renault 2008, Burge et al. 2014). One example is the pathogen of the hard clam *Mercenaria mercenaria*, long known as Quahog Parasite Unknown (QPX) and recently described formally as *Mucochytrium quahogii* Geraci-Yee & Allam, 2021 (Geraci-Yee et al. 2021). QPX can cause severe mortality events in hard clams, and although all evidence to date suggests that QPX is an opportunistic pathogen (Ford et al. 2002, Burge et al. 2013, Collier et al. 2017, Geraci-Yee 2021), many aspects of the disease and the QPX organism (*M. quahogii*) remain too poorly understood to confirm this theory or influence resource management decisions. While

*Corresponding author: bassem.allam@stonybrook.edu

Publisher: Inter-Research · www.int-res.com

the research required to gain such knowledge is ongoing for many marine pathogens, disease monitoring and surveillance programs with up-to-date and properly validated diagnostic tools are critical for supporting management and mitigation responses to marine disease outbreaks, including QPX disease.

Quantitative PCR (qPCR) has emerged as a benchmark technology for molecular disease diagnostics used to detect and quantify microbial pathogens (Johnson et al. 2013, Burge et al. 2016). qPCR assays have been developed for many bivalve pathogens, including QPX (Lyons et al. 2006, Liu et al. 2009), ostreid herpesvirus 1 (OsHV-1) (Burge et al. 2011), *Proctoeces maculatus* (trematode) in blue mussels (Markowitz et al. 2016), *Mikrocytos mackini* (mikrocytosis) in Pacific oysters (Polinski et al. 2015), *Perkinsus marinus* ('dermo' disease) in oysters (Gauthier et al. 2006, Ulrich et al. 2007, Faveri et al. 2009), *Perkinsus olseni* in clams (Ríos et al. 2020), *Haplosporidium nelsoni* (MSX disease) in oysters (Wilbur et al. 2012), and *Bonamia* spp. (bonamiosis) in the flat oyster (Ramilo et al. 2013). These diagnostic tools are most valuable when they are properly validated and documented in sufficient detail to be transferrable to other labs and used in combination with traditional methods such as histopathology to confirm infection and diagnosis (Burge et al. 2016). Although the World Organization for Animal Health (OIE) has established a Manual of Diagnostic Tests for Aquatic Animals (https://www.oie.int/en/what-we-do/standards/codes-and-manuals/aquatic-manual-online-access/) with methods of validation for nucleic acid detection tests, it lacks specific details on qPCR assay development, optimization, validation, and transparency in reporting that supports reproducibility among labs. The minimum information for publication of quantitative real-time PCR experiments (MIQE) guidelines (Bustin et al. 2009) and practical implementation of the guidelines (Bustin et al. 2010) can fill this gap. Unfortunately, these guidelines have yet to be widely recognized or adopted; in our example list of qPCR assays for bivalve disease diagnostics, we reviewed the six that were published after the establishment of the MIQE guidelines (Supplement 1; www.int-res.com/articles/suppl/d148p127_supp/) and found that only two (Wilbur et al. 2012, Polinski et al. 2015) referenced MIQE. Many of these publications were found to lack essential information needed for experimental transparency and reproducibility, with not a single publication covering all items deemed 'essential' by MIQE. We have found the MIQE guidelines very valuable, and one purpose of this paper is to make them more broadly accessible.

With decreased reliance on traditional histopathological methods and continual evolution of molecular tools for pathogen detection, it is important to continually assess, modify and diagnostically validate previously established molecular assays for pathogen detection (Carnegie et al. 2016, Groner et al. 2016). Assays developed before the implementation of the MIQE guidelines often lack the 'minimum information' described in MIQE as essential and fail to meet the minimum standards of assay functionality, such as the PCR amplification efficiency. This is the case for the QPX qPCR assay developed by Liu et al. (2009), which was a well-designed assay based on the scientific literature at the time its development began in 2006. However, its amplification efficiency of 82% (Liu et al. 2009) now fails to meet the general consensus that a reliable assay's PCR amplification efficiency should be at least 90% (e.g. 100 ± 10%) (Bustin et al. 2009, 2010, Johnson et al. 2013, Svec et al. 2015). Since the initial assay was developed, it has also been determined that the use of circular plasmid for standards results in serious overestimation of copy number abundance in qPCR (Dhanasekaran et al. 2010, Hou et al. 2010, Lin et al. 2011), and it is likely that any results obtained using the original assay reflect this overestimation. Additionally, according to the MIQE guidelines, sample inhibition should be assessed using dilutions of sample DNA template rather than an 'alien' spike, as used in the original assay.

The QPX qPCR assay represents the primary diagnostic tool used by the Marine Animal Disease Laboratory (MADL) at Stony Brook University for QPX disease monitoring of hard clams in New York (USA) for the past decade, being used to screen hundreds to thousands of clam samples each year and identify potentially infected clams (positive for QPX by qPCR), which are further evaluated by histopathology for confirmation of infection and intensity, representing the 'complementary' approach (Burge et al. 2016). In addition to the issues listed above with the original qPCR assay, any assay should be re-evaluated when changes are made to protocol, such as a change in equipment, reagents or kits, all of which have occurred in the MADL over the years. Therefore, we re-assessed, optimized and improved our QPX qPCR assay to incorporate recent advances and common practices in the qPCR approach for pathogen detection, in accordance with the MIQE guidelines. We also used our experience to develop a procedural roadmap (Fig. 1) and checklist (Table 1) we hope will help others to develop new assays or re-optimize, improve, or validate changes to existing

assays in a MIQE-compliant manner, because standardizing and streamlining bivalve pathology testing will provide better assessments and insights into pathogen distribution and prevalence necessary to effectively manage our valuable marine resources.

2. MATERIALS AND METHODS

2.1. Assay optimization

The QPX qPCR assay developed by Liu et al. (2009) was re-optimized according to the workflow described in Fig. 1, for the Mastercycler realplex[4] ep gradient S (Eppendorf) and realplex software (version 2.2) using twin.tec PCR 96-well, semi-skirted, colorless plates (Eppendorf), sealed with TempPlate RT Optical Film (USA Scientific). The assay used the same primers, 5.8S24For (17 bp: 5′-TTT AGC GAT GGA TGT CT-3′ at position 7–23 on the 5.8S rRNA gene of DQ641179) and QPX-ITS2-R2 (18 bp: 5′-GCC CAC AAA CTG CTC TWT-3′ at position 21–38 on the ITS2 rRNA region of DQ641179), which produce a 190 bp product (Fig. S1 in Supplement 2). Primers were synthesized by Integrated DNA Technologies, Inc. The original assay by Liu et al. (2009) used a SYBR green custom-made master mix, whereas this assay used Takyon No Rox 2× SYBR MasterMix blue dTTP (Eurogentec) in a 12.5 µl reaction. The qPCR cycling conditions remained the same as in Liu et al. (2009) for initial optimization trials (10 min at 95°C followed by 40 cycles of 30 s at 95°C, 1 min at 55°C, and 1 min at 72°C). Fluorescence was measured for individual wells at the end of each cycle with the detection threshold determined automatically by the qPCR software using the noiseband threshold and automatic baseline setting to determine quantification cycle or C_q values (also known at C_T values). Melt curve analysis was performed at the end of cycling to confirm the target amplicon. Additionally, for select samples gel electrophoresis and sequencing were also performed to confirm the expected size and sequence of the target amplicon.

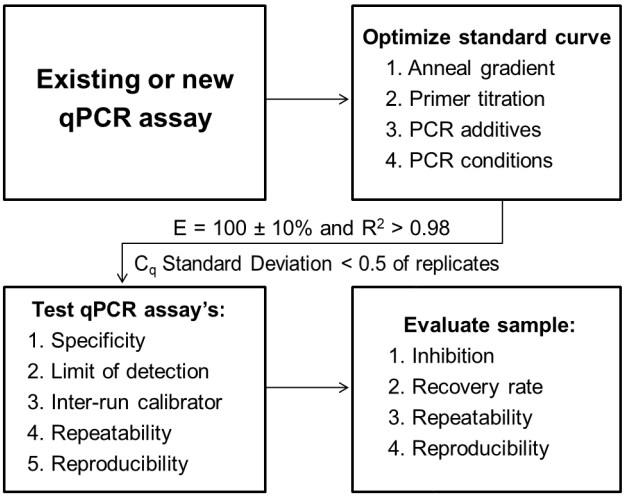

Fig. 1. Simple workflow for optimization of an existing or new quantitative PCR (qPCR) assay for absolute quantification. *E*: amplification efficiency; C_q: quantification cycle

The same plasmid developed by Liu et al. (2009), containing the QPX rRNA region amplified by QPX-F (5′-ATC CTC GGC CTG CTT TTA GTA G-3′) and 28S46Rev (5′-ATA TGC TTA ART TCA GCG GGT-3′), was used to construct the standard curve. Briefly, plasmid DNA was purified using the Wizard Plus SV miniprep DNA purification system (Promega), according to the manufacturer's protocols. The concentration of DNA was determined fluorometrically with a PicoGreen double-stranded DNA quantification kit (Molecular Probes) and a TBS-380 mini fluorometer (Turner Biosystemsto determine the proper amount to use in a restriction enzyme digest (approximately 1 µg of DNA). The circular plasmid was linearized using the restriction enzyme *Xmn*I (New England Biolabs), fast protocol with an incubation time of 10 min. *Xmn*I was selected as the restriction enzyme because it did not cut the plasmid insert and was located on the opposite side of the plasmid from the insert. Digested plasmid was run on a gel to confirm linearization and was gel-purified using the Wizard SV Gel and PCR Clean-Up System (Promega). Gel-purified, linearized plasmid was again quantified and copy number calculated using the conversion 10^9 copies μl^{-1} = 4.96 ng μl^{-1}, as determined by Liu et al. (2009). Linearized plasmid DNA was diluted to 10^8 copies μl^{-1} with nuclease-free water and stored in Axygen Maxymum Recovery microtubes (Corning) at −20°C to minimize degradation (Gaillard & Strauss 1998, Dhanasekaran et al. 2010). Linearized plasmid was routinely prepared fresh and used for only 1 mo. The linearized plasmid standard curve consisted of serial dilutions ranging from 10 to 10^6 copies. Dilution series were prepared using 10 µl of transfer volume into 90 µl of nuclease-free water, and each dilution was vortexed for 30 s and further mixed by pipetting before making the next dilution. Standards were stored at 4°C and discarded after 1 wk (Bustin et al. 2009, Dhanasekaran et al. 2010). The standard curve dilution series was used to optimize the assay based on amplification efficiency (E = 100 ± 10%) and linearity ($R^2 > 0.98$) (Bustin et al. 2009, Johnson et al. 2013). All reactions

Table 1. Modified quantitative real-time PCR experiments (MIQE) (Bustin et al. 2009, 2010) checklist for the new QPX quantitative PCR (qPCR) assay. ITS: internal transcribed spacer; C_q: quantification cycle; CV: coefficient of variation; IRC: inter-run calibrator; NTC: no template control; T_m: melting temperature; E: amplification efficiency

Assay checklist	Description
Sample/template	
Source	Hard clam whole mantle homogenate processed within 24 h
Method of preservation	Frozen at −80°C immediately after homogenization
Storage time (if appropriate)	DNA extracted within 1 yr after freezing
Extraction method	NucleoSpin Genomic DNA Tissue kit (Macherey-Nagel Inc.); QPX recovery rate = 30% (Table S12 in Supplement 2)
DNA storage	DNA stored at −20°C until assayed within 6 mo
Concentration/purity	Average = 27.8 ng μl^{-1} and $A_{260/280}$ = 1.98 by Nanodrop (Table S7, Fig. S4 in Supplement 2)
Inhibition assessment	Acceptable, PCR efficiency was within 10% of the standard curve assessed by dilution series of template DNA from a representative set of samples extracted with QPX cultured cells spiked into clam tissue homogenate (Tables S9–11 in Supplement 2)
Assay optimization/validation	
Sequence accession number	DQ641179, QPX isolate NY0400921C6; Fig. S1 in Supplement 2
Amplicon details	ITS region 190 bp; Fig. S1 in Supplement 2
Primer sequence	5.8S24For (5′-TTT AGC GAT GGA TGT CT-3′) and QPX-ITS2-R2 (5′-GCC CAC AAA CTG CTC TWT-3′); Fig. S1 in Supplement 2
In silico	See Liu et al. (2009)
Empirical	See Sections 2 & 3; Tables S2–S4 in Supplement 2
Priming conditions	Summarized in Fig. S3 in Supplement 2
Specificity	Tested against 7 other labyrinthulomycetes (see Sections 2 & 3); Table S6 in Supplement 2
PCR efficiency	PCR efficiency = 95% ± 1.89 SE; Fig. 2
Linear dynamic range	10 to 10^6 copies, R^2 = 0.993 ± 0.001 SE; Fig. 2 & Table S5 in Supplement 2
Limits of detection	10 copies (= 75 QPX copies mg^{-1} tissue or 0.17 QPX cells mg^{-1} tissue)
Intra-assay variation (repeatability)	Average C_q SD of standards = 0.43 ± 0.22 SD from 12 independent runs Average C_q SD of IRC = 0.18 ± 0.11 SD from 19 independent runs Average C_q SD of samples = 0.30 ± 0.20 SD for 423 samples
Inter-assay variation (reproducibility)	Average copy number CV = 0.11 ± 0.22 SD for 8 samples from 3 independent runs IRC copy number CV = 0.18 from 19 independent runs
PCR	
Protocols	See Section 2 and Supplement 3
Thermocycler	Mastercycler realplex^4 ep gradient S (Eppendorf)
Reagents	Takyon No Rox SYBR MasterMix dTTP Blue (Eurogentec); Fig. S3 in Supplement 2
Negative control	No amplification of NTC (no C_q or T_m)
Positive control	0.152 ng of QPX gDNA (used as IRC)
Replicates	All standards, samples, IRC, and NTC were run in at least triplicate
Inter-platform variation (reproducibility)	Assessed on QuantStudio6 Flex (Applied Biosystems); standard curve PCR E = 94.4% ± 0.65 SE and R^2 = 0.999 ± 0.0001 SE from 12 independent runs; average sample copy number CV = 24.8% ± 14.9 SD for 13 samples assessed by both platforms
Data analysis	
Software	Eppendorf realplex software (version 2.2), noiseband threshold and automatic baseline setting
Validation by histopathology	Yes, on a representative set of samples (Table S13 in Supplement 2)

were performed in at least triplicate (Svec et al. 2015).

An anneal gradient ranging from 45 to 65°C was performed to determine the anneal optimum for the thermocycler, as reaction temperatures may vary slightly between thermocyclers. A primer titration was performed using combinations of 50, 100, and 200 nM concentrations of forward and reverse primer, as suggested by the Takyon master mix technical data sheet. To test supplementation of the mas-

ter mix with the PCR additives and stabilizers used by Liu et al. (2009), varying combinations and concentrations of dimethyl sulfoxide (DMSO) and glycerol were compared, beginning with the final concentration used in the original assay of 3% DMSO (stored at room temperature in the dark) and 8% glycerol (from a 50% glycerol stock) added to the Takyon master mix.

2.2. Analytical specificity and sensitivity

QPX is a thraustochytrid and member of the labyrinthulomycetes. The original qPCR assay (Liu et al. 2009) was not tested for specificity, although the primers were tested for specificity *in silico* and using conventional PCR on 3 other thraustochytrids: *Aurantiochytrium limacinum* (ATCC MYA-1381), *Schizochytrium aggregatum* (ATCC 28209) and *Thraustochytrium aureum* (ATCC 34304). The new assay's specificity for QPX was tested on genomic DNA (gDNA) extracted from 7 cultured labyrinthulomycetes with the NucleoSpin Genomic DNA Tissue kit (Macherey-Nagel), following the manufacturer's protocol for cultured cells. The tested species belong to each of the 4 groups comprising the cultivated labyrinthulomycetes: labyrinthulids (*Labyrinthula* sp. isolate KIE13), aplanochytrids (*Aplanochytrium stocchinoi* isolate GSB06), oblongichytrids (*Oblongichytrium* sp. isolate 606), and thraustochytrids (the same 3 strains used previously plus *Japanochytrium marinum* ATCC 28207). Both melt curve and gel electrophoresis analyses were used to evaluate the assay's specificity. The sensitivity or limit of detection (LOD) of the original assay was reported as 10 copies per reaction (Liu et al. 2009). The LOD of the new assay was tested by determining the number of failed reactions at the lowest concentration of the standard curve. According to the MIQE guidelines, there should be no more than 5% failed reactions among all replicates at the LOD (Bustin et al. 2009).

2.3. Inter-run calibrator

Due to the large number of samples routinely analyzed using this assay, it is impossible for all samples to be run on the same plate and inefficient to run a standard curve on every plate as in the original assay. Therefore, an inter-run calibrator (IRC), also known as an inter-plate calibrator (IPC), was used to correct run-to-run differences (Bustin et al. 2010), and a single, highly precise standard curve was used for quantification (Svec et al. 2015). All C_q values, including the standard curve, were corrected by subtracting the IRC from the individual run and adding the average IRC value for all plates (Eq. 1) (Kubista 2010). Linearized standards and varying concentrations of QPX gDNA (single or mixed isolates extracted with the NucleoSpin Genomic DNA Tissue kit, see Assay Evaluation for QPX culturing details) run in at least triplicate were tested as the IRC to determine the most stable and robust calibrator.

$$C_q \text{ corrected} = C_q \text{ measured} - C_q \text{ calibrator} + \text{Average } C_q \text{ calibrators} \quad (1)$$

2.4. PCR setup and contamination controls

To minimize contamination, clam processing, QPX cultivation, DNA extraction, qPCR setup, and qPCR (thermocycler) were performed in separate rooms. Additionally, each step of the qPCR setup procedure was performed on a separate laboratory bench with designated equipment (pipettes, racks, tips, gloves, etc.). Plasmid standards and QPX gDNA were prepared on one bench (setup space 1) away from the qPCR reagents setup space (setup space 2, which was designated as DNA-free), and a third area was designated for loading sample template DNA into the qPCR plate (setup space 3). Filter pipette tips were used, and gloves were changed after handling any DNA (plasmid standards, QPX gDNA as the IRC, or sample template DNA). In each qPCR plate, at least 3 replicate negative controls (NTCs; no template) were included and if any of the NTCs resulted in amplification, the entire qPCR plate was considered invalid and the plate was repeated. The IRC was also used as a positive control. An example of the workflow follows: Before preparing the qPCR plate, all benchtop surfaces were disinfected with 10% bleach for 20 min, which was then removed with distilled water to eliminate any bleach residue. The benchtop and all equipment were then sprayed with 70% ethanol, which was allowed to fully evaporate. If the standard curve was being run, then it was prepared first in qPCR setup space 1 and stored at 4°C until loading. Then the qPCR master mix was prepared in qPCR setup space 2 and 11.5 µl of master mix was aliquoted to individual wells on the plate using a multichannel pipette, excluding the NTCs (no template). The plate was transferred to qPCR setup space 3, and 1 µl of sample template DNA was added to the appropriate wells in triplicate, including QPX gDNA (as the IRC) and plasmid standards (if

applicable). Reverse pipetting was used to ensure that the sample was dispensed and to avoid the production of bubbles and aerosols. Gloves were changed and then the NTCs were loaded (Bustin et al. 2010). After a plate was prepared, the qPCR setup area and equipment were again cleaned with 70% ethanol. Plates were sealed with adhesive optical film and spun down for 30 s at 280 × *g*. If bubbles were present in the wells, then the plate was spun again. In most cases, the plate was loaded into the qPCR machine immediately; however, sometimes plates were prepared and stored at 4°C for no more than 24 h (with no effect on results).

2.5. Assay evaluation

2.5.1. Clam processing and qPCR. Wild hard clams were collected using a bull or 'bubble' rake from a variety of sampling sites across Long Island, New York (USA), from May to October 2015 as part of a large-scale 2 yr survey of QPX disease (Fig. S2 in Supplement 2). Clams were insulated by bubble-wrap and put on ice for transport back to the laboratory, where clams were washed, measured and processed within 24 h. The clams were dissected, and a thin cross-section of clam meat, containing mantle, siphon, gills, digestive glands, stomach, gonad, pericardium and kidney, was fixed in 10% buffered formalin to be used for histological examination (Howard et al. 2004). To avoid false negatives arising because focal infection sites typical of QPX disease were excluded by chance from small tissue biopsies, the rest of the mantle and siphon was collected, gently blotted, and weighed. Ten times the clam tissue weight of 1× phosphate-buffered saline (PBS) was added, and the tissue sample was homogenized using a GMBH Polytron benchtop homogenizer (Kinematica AG) on medium speed (<5) until the tissue was easily pipetted through a Finntip wide orifice pipette tip (Thermo Fisher Scientific). The mantle tissue homogenate was aliquoted into 2 subsamples, 200 µl and 1 ml, and stored at –80°C. The 200 µl aliquot of homogenized tissue sample (equivalent to 20 mg of tissue) was used for DNA extraction, while the 1 ml sample was kept for reserve. The 200 µl aliquot was thawed, vortexed, and centrifuged at 12000 × *g* for 10 min to remove the supernatant (PBS). DNA was extracted from the clam tissue pellet with the NucleoSpin Genomic DNA Tissue kit (Macherey-Nagel), using the standard protocol for animal tissue. Samples were incubated overnight for pre-lysis (16–18 h) and processed further by following the manufacturer's protocols. DNA was eluted for high yield by using pre-warmed elution buffer (70°C) that was incubated on the spin filter for 3 min at room temperature and 2 elutions of the spin column, 75 µl each, for a total elution volume of 150 µl. DNA concentration and purity was evaluated using Nanodrop ND-1000 spectrophotometry (Thermo Scientific). All DNA was extracted within 1 yr of sample collection and DNA was stored at –20°C until being used in the qPCR assay.

Triplicate qPCR reactions were performed on each sample using 1 µl of sample DNA as template. Samples that had a C_q value and appropriate melt curve peak temperature (T_m) but were below the LOD were considered positive and denoted as below the LOD (BLD), since they were not truly negative but also could not be accurately quantified. C_q values were only accepted if the standard deviation (SD) was less than 0.5 for at least 2 of the 3 replicates; usually SDs >0.5 were due to one outlier, which when removed resulted in an acceptable C_q SD. Samples that did not meet this criterion were rerun until replicates agreed (usually rare), unless they were designated as BLD. Weighted prevalence was determined based on the sum of QPX load rated on an intensity scale (Table S1 in Supplement 2) for each individual clam, divided by the number of clams assayed for each sampling event or cohort. QPX prevalence, weighted prevalence, and concentration in hard clam tissues were visualized using Microsoft Excel or ggplot2 (Wickham 2016) in RStudio v1.2.1335 (RStudioTeam 2018).

2.5.2. Converting rDNA copy number to cellular concentration. The DNA content of QPX cells was determined by Liu et al. (2009) in order to convert QPX copy number to QPX cell number (Galluzzi et al. 2004), assuming that the rDNA copy number of QPX cells in culture is similar to that of QPX in clams. Since QPX cells in clam tissue and in culture usually contain multiple nuclei, varying with cell size and life stage (Geraci-Yee 2021, Geraci-Yee et al. 2021), this procedure was repeated with the addition of a DAPI (4′,6-diamidino-2-phenylindole) staining step to determine DNA content per nucleus using a geographically representative mixture of 4 QPX isolates, 2 from New York (8BC7 = ATCC TSD-50 and 20AC1), 1 from Massachusetts (MA; ATCC 50749), and 1 from Virginia (VA) (Geraci-Yee et al. 2021). The 4 QPX isolates were individually cultured in modified minimal essential medium (MEM) supplemented with 10% fetal bovine serum (FBS) (Kleinschuster et al. 1998) or ATCC medium 2126, at room temperature on an orbital shaker at low speed to reduce mucus pro-

duction. Cultures were pooled and harvested while they were in the active growth phase (5 to 7 d). An equal volume of 1× PBS was added to the pooled culture, and the mucoid material enveloping the cells was removed by washing and trituration (slow passage through a 20 gauge needle), known as 'demucusing' (Qian et al. 2007, Geraci-Yee et al. 2021), followed by centrifugation at 2500 × *g* for 5 min. The cell pellet was resuspended in 1× PBS, and the trituration/spinning/washing process was repeated 5 to 10 times until all traces of mucus were removed. The demucused culture was centrifuged at 2500 × *g* for 30 min, and the cell pellet was resuspended in 5 ml of 1× PBS. Cells were then separated into <5 and >5 µm fractions. The <5 µm cell fraction was obtained using a syringe and 5 µm in line filter to remove cells larger than 5 µm. The >5 µm fraction was obtained using a 5 µm filter and filter apparatus under low pressure (~1 mm Hg) to remove cells smaller than 5 µm, then resuspending the >5 µm cells from the filter into 1× PBS.

To determine nuclei per cell in each size fraction, a 100 µl aliquot of cells was mixed with a final concentration of 0.8% formaldehyde by pipetting and incubated at room temperature for a minimum of 30 min. An aliquot of 20 µl of fixed cells was mixed with 10 µl of DAPI (1 µg ml^{-1} in de-ionized distilled water, ddH_2O) by pipetting and incubated in the dark at room temperature for at least 10 min. Cell size and nuclei per cell were determined for a minimum of 50 cells from each size fraction using a Leitz Laborlux S fluorescence microscope equipped with a Lietz A filter cube (excitation BP 340-380 nm; dichroic 400 nm; emission LP 425 nm). For DNA extraction, a 1 ml aliquot from each size fraction was spun down and resuspended in 1 ml of lysis buffer (10 mM Tris-HCl pH 8, 50 mM KCl, 0.5% Nonidet P40, 0.5% Tween 20, 0.1 mg ml^{-1} Proteinase K in sterile ddH_2O). A 10 µl sample was removed to determine cell concentration using a hemocytometer (Hausser Scientific), and a minimum of 200 cells were counted. The remaining sample was placed on ice for 30 min. Samples were sonicated using a VirTis Virsonic 50 at 50% power (setting 12–13) for 20 s using a cold rack, while lifting the sample up and down slowly but keeping the probe submerged. This was repeated a total of 3 times with 1 min incubations on ice in between sonication rounds. During initial testing of methods, cells were visually inspected before each round of sonication to monitor the extent of cell disruption, and 3 rounds of sonication left no intact cells. After sonication, the sample was vortexed and incubated at 60°C for 3 h with vortexing every 30 min for 10–20 s. Samples were then placed on ice for 30 min to precipitate cell debris and centrifuged at 12 000 × *g* for 10 min to recover supernatant, which contained crude lysate DNA. This DNA was quantified by PicoGreen at least in triplicate to determine DNA concentration per cell. DNA concentration per cell divided by nuclei per cell was used to determine DNA content per nucleus. Two independent trials with a total of 4 replicates from the <5 µm fraction and 2 replicates from the >5 µm fraction were performed. Finally, using the estimated DNA content per nucleus, a secondary standard curve of mixed QPX gDNA serial dilutions was run in the qPCR assay to determine copy number in 3 independent trials. The number of copies in each dilution was plotted against DNA content per nucleus to determine the number of copies per QPX nucleus.

2.5.3. Inhibition testing. Due to the large number of samples that are routinely screened for QPX using this assay, it is impractical to test each sample for inhibition by either single-point alien spike (e.g. addition of a known amount of QPX plasmid as in the original assay) or serial dilution series. Therefore, inhibition testing was carried out on a representative set of samples, by season and site (Bustin et al. 2010). After qPCR, one positive (quantifiable), one BLD (positive, unquantifiable), and one negative sample from each Birch Creek sampling time point were selected to determine if inhibition varied seasonally, and at least one positive, quantifiable sample from each sampling site was selected to determine if inhibition varied by site. Since there were no samples with enough QPX to perform the dilution series spanning several orders of magnitude needed to assess amplification efficiency, cultured QPX cells were spiked into a new 200 µl aliquot of homogenized mantle tissue for the selected samples. A mix of cultured QPX isolates was prepared and demucused as described above, re-suspended in 1× PBS and counted using a hemocytometer. Approximately 10^6 cells were added to the tissue homogenate, from which DNA was extracted using the same procedure as the original 'unspiked' samples. The purified DNA was used to create a C_q dilution series in the same way as the standard curve, using 10 µl transfer volume. We also tested a serial dilution of QPX gDNA from the same mixed culture. Sample amplification efficiencies and linearity were calculated, and the efficiency was considered acceptable, indicating minimal PCR inhibition, if it was within 10% of the efficiency of the standard curve (Irwin et al. 2012) with an $R^2 > 0.98$ (Johnson et al. 2013).

2.5.4. Recovery of QPX. The recovery rate (percent) of QPX DNA was estimated by comparing the QPX concentration determined from the spiked samples used in inhibition testing with unspiked samples from the same clams using Eq. (2). Samples were spiked with 10^6 QPX cells, represented by 'QPX added' in Eq. (2).

$$\text{Recovery rate (\%)} = (\text{QPX spiked} - \text{QPX unspiked}/\text{QPX added}) \times 100 \quad (2)$$

2.5.5. Inter-platform reproducibility. As an additional measure of reproducibility, we assessed the performance of the new qPCR assay on the QuantStudio6 Flex using QuantStudio Realtime PCR Software v1.2 by Applied Biosystems. The standard curve and a subset of samples (n = 22) consisting of QPX-positive, BLD and negative samples were assessed following the same protocol as described here with the addition of ROX (Eurogentec) as passive dye to the Takyon master mix (2.8 µl per 1 ml of Takyon) and the use of 384-well plates (MicroAmp Optical 384-well reaction plate and optical adhesive film, Applied Biosystems, ThermoFisher Scientific). Cycling parameters were kept as similar as possible by using the QuantStudio6 Flex maximum ramp rates (heating = 2.252°C s^{-1} and cooling = 1.92°C s^{-1}), compared to the Eppendorf Mastercycler realplex[4] default ramp rates of 6 and 4.5°C s^{-1} for heating and cooling, respectively. Additionally, the melt curve stage was modified from the default on the QuantStudio6 Flex to 0.029°C s^{-1} to match the 20 min stage on the Eppendorf machine. The software used auto threshold and baseline settings for the determination of C_q values.

2.5.6. Histopathological analysis. Histopathology was performed as described by Liu et al. (2017) on all samples >1000 copies mg^{-1} tissue or the sample with the highest signal from each site, as well as some BLD and negative samples from Raritan Bay, for confirmation of diagnosis (QPX infection) and assay validation. The histology cassettes were embedded in paraffin, sectioned at 5–6 µm, mounted on slides, stained (H&E; Harris' haematoxylin for 2 min and Eosin Y for 1 min), and examined using light microscopy.

3. RESULTS

3.1. Assay optimization

Assay conditions were tested for acceptable qPCR parameters, where the PCR efficiency (E) is 100 ± 10% (range of 90–110%), equivalent to a slope of 3.1–3.58, with a linearity (R^2) > 0.98 using the standard curve of linearized plasmid serial dilutions from 10 to 10^6 QPX copies. This qPCR assay was robust, with acceptable performance over a range of conditions tested (Tables S2–S4 in Supplement 2), which meant many optimization decisions were based on fine distinctions. We wanted the most robust assay possible and therefore aimed to achieve efficiency as close to 100% (but not above) and linearity as close to 1 as possible, with the smallest intra- and inter-run variance.

3.1.1. Anneal temperature. Temperature gradient analysis of the standard curve (without any PCR additives) revealed successful amplification over a wide range of primer annealing temperatures from 45 to 62°C (Table S2 in Supplement 2). Linearity (R^2) of the standard curve was suboptimal for all temperatures tested with flattening of the regression line toward the lower concentrations (10 and 100 copies). Poor linearity may have resulted from the use of only 1 replicate per concentration due to the machine gradient setting, in which each column is a different temperature. This was the only trial that did not use at least 3 technical replicates. Based on the amplification efficiency and linearity, the temperature gradient analysis suggested the anneal optimum to be between 53.9 and 56.5°C, with higher temperatures resulting in efficiencies over 100%. Since the original assay by Liu et al. (2009) was performed at an anneal of 55°C, we further compared the anneal temperatures of 54 and 55°C in 3 independent trials. There were no significant differences between the 2 anneal temperatures, although there was a tendency for lower anneal temperature to produce a slightly better amplification efficiency (closer to 100% with an average difference of 3.58 ± 2% SD). We therefore used 54°C as the anneal temperature for the remaining optimization trials.

3.1.2. Assay reagents. For most of the primer concentrations tested (Table S3 in Supplement 2), the PCR efficiency was within acceptable limits, while the linearity was suboptimal for all but the 100 nM forward/reverse trial, which is the same concentration used in the original assay by Liu et al. (2009) and therefore did not require further testing. Different combinations and concentrations of PCR additives and stabilizers were added to the Takyon master mix and evaluated based on the qPCR parameters (Table S4 in Supplement 2). The optimal set of additives was 1% DMSO and 8% glycerol, which improved linearity with efficiencies within the accepted range. We also re-examined the qPCR cycling conditions and

found that reducing the extension time from 1 min to 30 s had no apparent effect on efficiency or linearity, so we reduced the extension time to reduce overall assay run time. The final qPCR reagents and cycling parameters (10 min at 95°C followed by 40 cycles of 30 s at 95°C, 1 min at 45°C, and 30 s at 72°C followed by melt curve analysis), determined from these optimization trials and used for the rest of the study, are shown in Fig. S3 in Supplement 2.

3.2. Assay performance

We assessed assay performance as efficiency and linearity of the standard curve over 12 independent trials each with at least 3 technical replicates (Fig. 2). The average PCR efficiency was 95% with a range of 86–107%. This was a marked improvement from the original assay of Liu et al. (2009), which had an efficiency of 82%. All qPCR parameters were in compliance with the MIQE guidelines.

3.2.1. Analytical sensitivity and reproducibility. All but the lowest concentration of the standard curve, spanning 5 orders of magnitude, had an inter-run C_q SD at most 0.539 and a SE at most 0.163, indicating excellent reproducibility (Table S5 in Supplement 2). At the lowest concentration (10 copies), the inter-run SD of C_q values was slightly higher than desirable at 0.82. The sensitivity or LOD of the assay was 10 copies per reaction with no failed reactions (88 replicates over 20 plates, including optimization trials).

3.2.2. Analytical specificity. The assay's specificity was tested on representative species from the 4 cultivated labyrinthulomycete groups. The assay only produced a product using template gDNA from thraustochytrids and not the other groups of labyrinthulomycetes (oblongichytrids, aplanochytrids, labyrinthulids) (Table S6 in Supplement 2). Melt curve and gel electrophoresis analyses revealed different melting temperatures and larger products (>200 bp) from the other thraustochytrids compared to the targeted QPX product (Table S6). There was no amplification in the negative control (no template DNA), suggesting that no contamination occurred in this test.

3.2.3. Inter-run calibrator (IRC). The linearized plasmid standards were too unstable to be good candidates for the IRC. In addition, creating fresh dilutions for virtually each run, as linear standards are only viable for 1 wk (Bustin et al. 2009), proved to be inefficient. QPX gDNA provided a better candidate for the IRC, as it was found to be extremely stable long-term, even at low concentrations. There was also no difference observed between using gDNA of a single QPX isolate or several isolates. Therefore, we used pooled gDNA from the 4 isolates previously mentioned. Serial dilutions of QPX gDNA, spanning 8 orders of magnitude from 15.2 ng μl^{-1} to 1.52 fg μl^{-1}, were tested as potential IRCs. We narrowed our choices for the IRC to 3 concentrations, 152, 15.2 and 1.52 pg μl^{-1} of QPX gDNA, which had a C_q range of 19–26. The most stable and consistent concentration was 152 pg μl^{-1} (0.152 ng μl^{-1}) of QPX gDNA. This IRC was run across 19 plates in triplicate with an inter-run average C_q of 19.74 ± 0.07 SE and 0.29 SD.

3.2.4. Standard curve. A highly precise, robust standard curve consisting of 8 replicates was run, and C_q values were corrected using the IRC. The replicates had excellent intra-run repeatability with SDs less than 0.5 for each concentration, and the standard curve had a qPCR efficiency of 93% and linearity of 0.997. The IRC C_q corrected standard curve was used to convert sample C_q corrected values into QPX copy number using Eq. (3).

$$\text{QPX copy number} = 10^{(C_q \text{ corrected} - 38.882)/-3.5017} \quad (3)$$

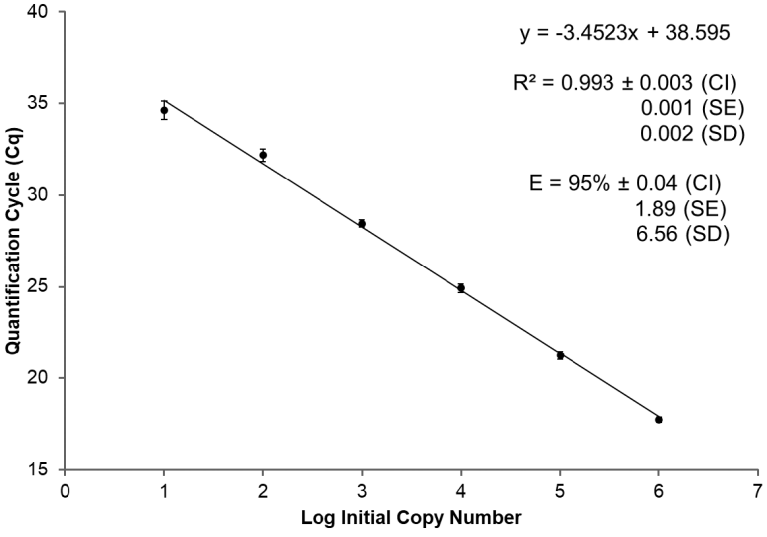

Fig. 2. Standard curve of linearized plasmid serial dilutions from 10 to 10^6 QPX copies averaged over 12 independent trials with 95% confidence intervals (CI). Each trial consisted of at least 3 replicates. Amplification efficiency (E) and linearity (R^2) are expressed as the mean with CI, SE, and SD

3.3. Assay evaluation

Wild hard clams were collected from 7 sampling sites around Long Island, NY, from May to October 2015 (Fig. S2 in Supplement 2). Ten to 20 of the 30 clams collected from each sampling trip were randomly selected, for a total of 423 clam samples that were screened for QPX using the new assay. The DNA concentration (ng μl^{-1}) and purity ($A_{260/280}$) had an overall average of 27.8 and 1.98, respectively (Table S7 in Supplement 2). The average C_q SD of clam replicate samples was 0.3 ± 0.2 SD, showing that the assay was acceptable in terms of repeatability or intra-assay variation (Bustin et al. 2009). Raw C_q values were corrected by the IRC using Eq. (1). The IRC calibration or C_q correction of the 347 positive samples (82% positive of 423 assayed) run across 18 plates altered the C_q value on average by 0.04, showing that the run-to-run variation was less than the accepted SD of replicate C_q values (SD < 0.5). There was a weak linear relationship between corrected C_q values and DNA concentration or purity (Fig. S4 in Supplement 2). We also tested the inter-run variance of some of the highest positive clam samples (i.e. samples with the lowest C_q value; n = 8) and found that run-to-run differences were removed by the IRC technique, resulting in C_q SDs less than 0.5 between different runs of the same sample. From the mean corrected C_q value of each sample, the QPX copy number was determined using Eq. (3). The number of copies per mg clam tissue was determined using Eq. (4), where the elution volume of the extracted DNA was equal to 150 µl from 20 mg of hard clam mantle tissue.

$$\text{QPX copies mg}^{-1}\text{ tissue} = \frac{(\text{QPX copy number} \times 150\ \mu\text{l})}{20\ \text{mg tissue}} \quad (4)$$

Melt curve analyses of qPCR products from clam tissue samples revealed a single peak at 79.5°C (Fig. S5 in Supplement 2), which was the same observed T_m of both QPX gDNA and plasmid standards. qPCR products of several positive clam samples were analyzed by gel electrophoresis, revealing a single band at approximately 190 bp (Fig. S5 in Supplement 2). The bands were gel purified and sequenced, confirming the target QPX product in all cases (>99% sequence identity). Of the 423 clams assayed, 31% were positive and quantifiable, 51% were positive, but BLD and 18% were negative. QPX prevalence and weighted prevalence were determined for each sampling cohort (Fig. 3). QPX prevalence ranged from 56 to 100% with an average of 82% ± 14 SD, and QPX weighted prevalence ranged from 0.63 to 2.13 with an average of 1.19 ± 0.43 SD, which is considered 'light' on the QPX intensity scale (Table S1 in Supplement 2). QPX copies mg^{-1} tissue of the positive–quantifiable samples (n = 131) ranged from 75 to 8845 with an average of 397 ± 1053 SD (Fig. 3). QPX was detected and quantified in clam samples from every sampling event, except at the Birch Creek sampling site in October, when all samples were either BLD or negative. There was no difference in QPX prevalence (% total positive, positive, BLD, and negative) or weighted prevalence of clam samples by site, month, or QPX disease history (Table S8 in Supplement 2).

3.3.1. Converting to cellular concentration. There was a direct relationship between QPX cell diameter and number of DAPI-stained nuclei (cell diameter µm = 0.991 (no. of nuclei) + 4.457, $R^2 = 0.753$) (Geraci-Yee et al. 2021). The average cell diameter and number of nuclei of the <5 µm fraction cells were 3.5 µm and 1.3 nuclei, compared to 9.6 µm and 6 nuclei in the >5 µm fraction. DNA content per nucleus was 55.96 ± 2.95 fg (average ± SD of 6 determinations), with no difference between the 2 fractions. Using the secondary standard curve of mixed QPX gDNA, the number of rDNA target copies per nucleus averaged 440 ± 32 copies (SD) from 3 independent trials. The conversion from QPX copies into number of single-nucleated QPX cells (referred to as QPX cells) is presented in Eq. (5) with a LOD of 0.17 QPX cells mg^{-1} tissue. The QPX cellular concentration range of the positive–quantifiable clam samples was 0.171 to 20.1 cells mg^{-1} tissue with an average of 0.9 ± 2.4 SD.

$$\text{QPX cells mg}^{-1}\text{ tissue} = \text{QPX copies mg}^{-1}\text{ tissue}/440 \quad (5)$$

3.3.2. Inhibition. Eleven samples from Birch Creek were used to assess seasonal inhibition in positive, BLD, and negative samples (Table S9 in Supplement 2). The average PCR efficiency for positive samples was 89.27%, BLD was 89.5%, and negative was 86.72%. The average PCR efficiency for these samples by sampling month ranged from 86 to 91%. Seven additional positive samples were assessed for inhibition from each sampling site (Table S10 in Supplement 2). The average PCR efficiency of these samples was 88.33% with a range from 84–91%. All samples had a linearity >0.97 (Tables S9 & S10 in Supplement 2). There were no differences in efficiency or linearity by sampling month, qPCR result, or site (Kruskal-Wallis rank sum test, Table S11 in Supplement 2), although efficiency of the negative samples was slightly lower than positive–quantifiable and

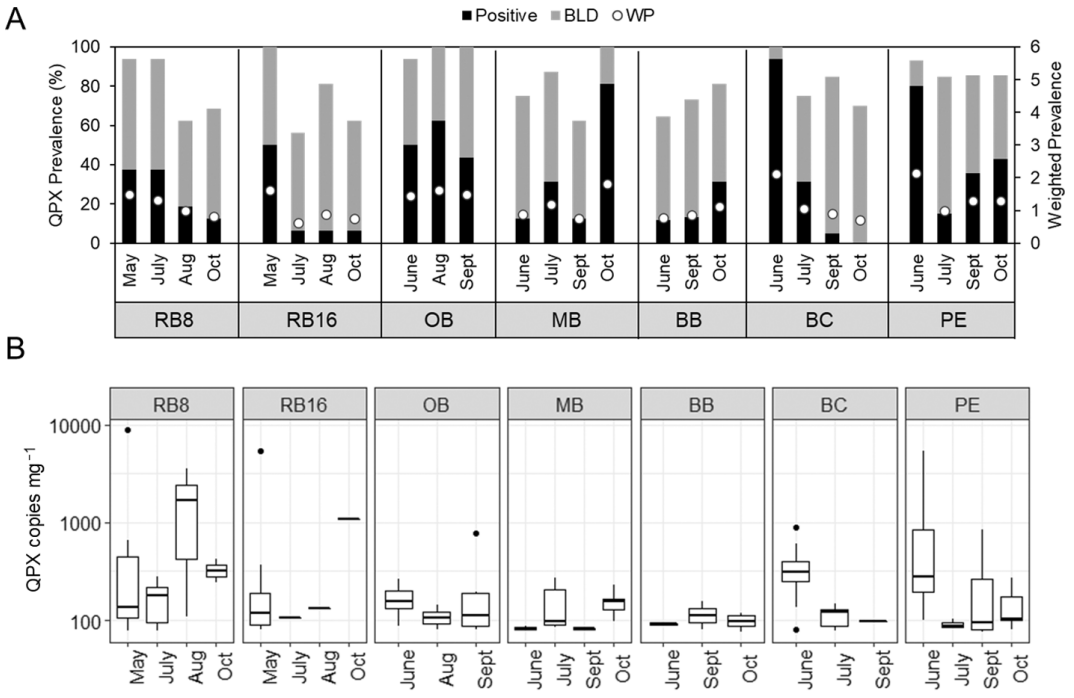

Fig. 3. (A) QPX prevalence (%) and weighted prevalence (WP) in hard clam tissue samples as determined by quantitative PCR (qPCR) by sampling site and month. BLD (below limit of detection) represents samples that were positive but could not be accurately quantified. The percentage of positive–quantifiable and positive–BLD samples represent total QPX prevalence. (B) Box plots of QPX abundance in gene copies mg^{-1} tissue of positive–quantifiable hard clam tissue samples on a logarithmic scale. RB: Raritan Bay; OB: Oyster Bay; MB: Moriches Bay; BB: Babylon Bay; BC: Birch Creek; PE: Peconic Estuary (Fig. S2 in Supplement 2). Sites RB, OB, and BC are areas where QPX disease in clams has been previously identified. Sites BB, MB, and PE are areas that have never been screened for QPX. RB had 2 subsites (8 and 16)

positive–BLD samples. These values are remarkably similar to the qPCR performance measured in QPX gDNA of 90.5 ± 0.9% SD with linearity of 0.998 ± 0.002 SD determined from 3 independent trials.

3.3.3. Recovery of QPX. The positive samples that were used in determining inhibition (from above) were also used to determine the recovery rate of QPX through the DNA extraction kit and qPCR assay (Table S12 in Supplement 2). The recovery rate varied from 13.72 to 51.1% with an average rate of 29.74% ± 11.52 SD.

3.3.4. Inter-platform reproducibility. The assay functioned similarly on the Applied Biosystems QuantStudio6 Flex in 384-well format as the Eppendorf Mastercycler realplex^4 in 96-well format. The standard curve PCR efficiency was 94.4% ± 0.65 SE and R^2 = 0.999 ± 0.0001 SE from 12 independent trials. The C_q values were shifted approximately 5 C_q earlier on the QuantStudio6 compared to the Eppendorf Mastercycler. The melt curve peak was observed at a T_m of 79.5°C, which was the same T_m for the Eppendorf Mastercycler. The IRC C_q value averaged 14.61 ± 0.03 SE over 12 independent trials, with at least 3 technical replicates in each trial. A total of 22 samples were assayed on the QuantStudio6: 13 of 13 samples were QPX-positive between the 2 machines, 1 of 1 was negative, and 5 of 8 were BLD (i.e. only 5 of 8 tested BLD samples were BLD on the QuantStudio6). The other 3 BLD samples did not contain the QPX target and instead had a melt curve peak (T_m) around 75–77°C; when visualized on a gel, there was an extremely faint, wide, diffuse band around 350–400 bp. This larger band was also seen in the negative sample, which had a T_m of 77°C but no C_q value. The average copy number coefficient of variation (CV) of positive samples assessed by both machines was 24.8% ± 14.9 SD, representing approximately 25% variation between the 2 platforms.

3.3.5. Histopathological analysis. A total of 41 samples were processed for histopathology, representing approximately 10% of the total samples assayed by qPCR. Of these samples, 31 were positive, 9 were BLD, and 1 was negative by qPCR. BLD samples and the negative sample were negative by histopathology, while 4 of the 31 positive samples by qPCR were also positive by histopathology (~13%). The 4 samples that were positive by histopathology

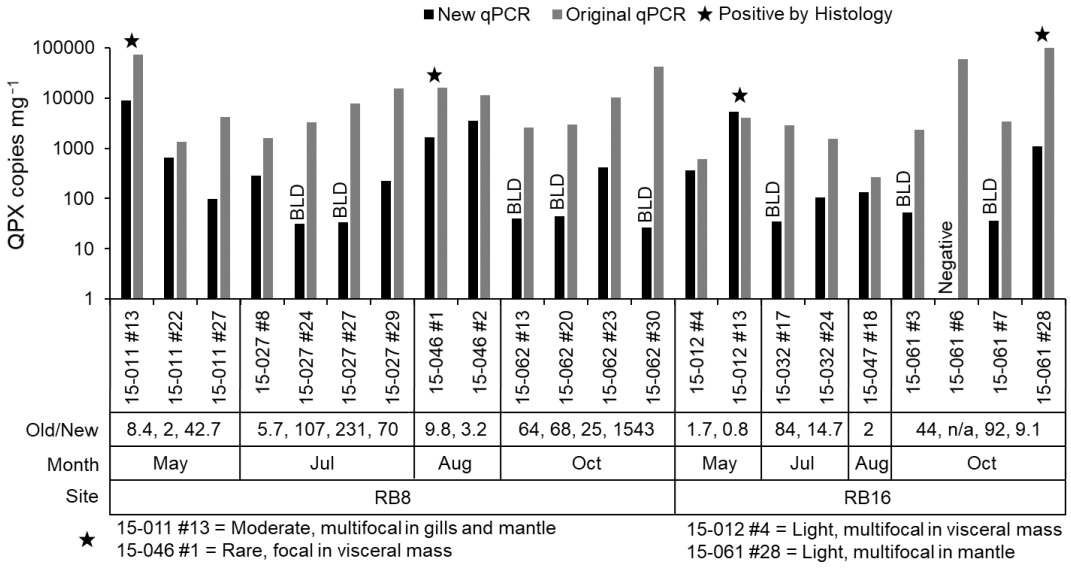

Fig. 4. Comparison of QPX concentration determined by the original and new quantitative PCR (qPCR) assay performed on the same biological samples (n = 22) from 2 Raritan Bay (RB) sampling sites from May, July, August and October on a $\log_{10}$ scale for visualization. Overestimation by the original assay (Liu et al. 2009) is shown as 'Old/New'; on average the old assay overestimated QPX concentration by 115.6 times ± 331.6 (SD)

were all from Raritan Bay (Fig. 4, Table S13 in Supplement 2) and ranged in intensity from rare to moderate with QPX lesions located in the mantle, gills, and visceral mass. QPX concentration determined by qPCR for those 4 samples ranged from 1093 to 8845 QPX copies mg^{-1} tissue (= 2.5–20.1 QPX cells mg^{-1}). None of the samples from the other sampling sites were positive by histopathology (Table S13 in Supplement 2).

4. DISCUSSION

4.1. Assay optimization and performance

Through the assay re-optimization process, 19 significant changes were made to the original qPCR protocol of Liu et al. (2009), which are summarized in Table S14 in Supplement 2. The most important outcome is improved PCR efficiency, which now is in accordance with current qPCR guidelines (Bustin et al. 2009, 2010, Johnson et al. 2013). The lowest efficiency obtained from this assay during testing was 86%, with an overall average efficiency of 95% for the linear plasmid standard curve (Fig. 2). There are several factors contributing to this improvement. One is the change in plasmid DNA conformation used for the standard curve from circular to linear. There is a trade-off when using linear standards, as they are much less stable than the circular form, which could lead to changes in copy number and therefore absolute quantification over time. However, proper handling and storage of linear plasmid (see Section 2) help to minimize this problem, as does the construction of one very precise standard curve and using the IRC instead of a standard curve on each plate to account for inter-run variation. Another factor contributing to the improved efficiency may be the change in anneal temperature to 54°C rather than 55°C. Finally, the optimization of the Takyon master mix with PCR additives and stabilizers (DMSO and glycerol) also contributed to the assay's improved PCR efficiency, linearity, repeatability, and reproducibility.

Another important aspect of this assay improvement is the development of detailed protocols for contamination control. At the beginning of our trials, contamination was frequent with at least 1 QPX-positive replicate NTC reaction on each plate. It was not until the thorough cleaning and decontamination of work areas and equipment, designation of separate rooms and/or laboratory bench spaces, and implementation of the protocols described in Section 2.4 that contamination was no longer present in the NTCs. Of the 18 plates used to assay the clam tissue samples reported here, only 1 plate had to be repeated due to amplification in one of the 3 NTCs. Establishing specific, detailed protocols can ensure quality control between different runs, personnel, and laboratories; a detailed protocol for this assay is provided in Supplement 3.

The re-optimized qPCR assay was validated for analytical sensitivity and specificity, as well as repeatability (intra-run assay variance) and reproducibility (inter-run assay variance). While there were no failed reactions at the LOD of 10 copies, the C_q SD and SE values at this concentration were slightly higher than the rest of the standard curve C_q inter-run variance without using the IRC technique (Fig. 2, Table S5 in Supplement 2). This higher variance at the lowest concentration was not considered unusual because at low copy numbers, stochastic events can have a larger effect on C_q, resulting in higher variance (Bustin et al. 2009), as well as potential degradation of the linear plasmid over time. In terms of specificity, template gDNA from other thraustochytrids did amplify, but their products were larger and could be easily identified by melt curve analysis (Table S6 in Supplement 2; T_m was higher compared to the QPX T_m). While the forward primer was designed, based on sequences available at the time, to be specific for QPX by Liu et al. (2009), it does match (100% ID) to some of the other labyrinthulomycetes, as well as some eukaryotes (e.g. fungi, dinoflagellates, and apicomplexans). We speculate that the production of these larger products is due to the lack of specificity of the forward primer; however, in the clam samples surveyed, these larger products were never observed when using the Eppendorf Mastercycler. Clam samples assayed using the QuantStudio platform that were BLD and negative on the Eppendorf platform did contain a larger non-specific product with a T_m lower than the QPX T_m. Unfortunately, when visualized on a gel the band was so faint that we were not able to isolate and sequence it. We are not sure if this larger product is the same product seen during specificity testing with other labyrinthulomycetes since they had different melt temperatures. We think this larger band found in these clam samples may arise due to the lower temperature ramp rate of the QuantStudio compared to the Eppendorf machine, resulting in non-specific amplification when the QPX target is absent or low. Samples that contained QPX and could be accurately quantified (within the standard curve) performed well on the QuantStudio, while BLD samples exhibited variability between the 2 machines. It is not unexpected that there would be inter-platform variability for BLD samples, since they sometimes exhibited intra-run variability (C_q SD > 0.5). Additional optimization may be required to reduce this inter-platform variability, as once positive BLD samples would be considered negative after melt curve analysis, altering the total QPX prevalence (qPCR positive and BLD samples). However, since low-target reactions are dictated by stochastic processes, it may not be possible considering the limits of the QuantStudio platform's temperature ramp rates. The detection of these low-target samples may only be achieved with platforms with similar ramp rates to the Eppendorf machine.

Other important changes to the assay have made it less time-consuming and more cost-effective. In particular, the use of the IRC technique removes the need to run a standard curve on each plate, allowing more samples to be run in triplicate on a single plate, reducing the potential for having to rerun samples due to large variation between duplicate C_q values. In cases where the standard deviation among 3 replicates was unusually large, it was most often due to a single 'outlier' reaction and the standard deviation between the remaining 2 replicates was acceptable to complete the analysis (SD < 0.5) after removal of the outlier. The IRC technique also reduces the time it takes to prepare a plate by almost 30 min, as a standard curve dilution series does not need to be prepared for each plate. Although run-to-run variation for this assay was determined to be minimal, perhaps reflecting its general robustness, the IRC technique can correct for run-to-run variation (Bustin et al. 2010, Kubista 2010) and allows all samples to be quantified using one highly replicated version of the standard curve (Svec et al. 2015). However, it is advised that a new standard curve be performed when a new batch of IRC is prepared or there is an observed C_q shift of >1 C_q from the average IRC C_q value. Additionally, with a reduction of PCR extension time, the assay is approximately 20 min shorter in thermocycler run time compared to the original assay (Liu et al. 2009). Overall, the qPCR assay can be completed within 2.5 h. The run time may even be further shortened on the QuantStudio platform, as the C_q values were shifted, suggesting the assay could be shortened to 35 cycles instead of 40. Furthermore, use of the 384-well plate on the QuantStudio platform further increases efficiency, allowing for over 100 samples to be assayed in one run. All of these aspects save time and money, which become increasingly important when an assay is used to screen the hundreds to thousands of samples often necessary for disease surveillance and monitoring.

4.2. Assay evaluation and application

Although both the original and improved versions of the assay have a LOD of 10 copies per reaction, the

reported minimum concentration of QPX (cells mg^{-1} tissue) detected differs: in the original assay by Liu et al. (2009), the theoretical LOD was 0.08 QPX cells mg^{-1} tissue, while in the new assay is 0.17 QPX mononucleate cells mg^{-1} tissue. There are 2 reasons for this difference: (1) change in the mass of starting material used for the DNA extraction and (2) the conversion factor used to convert from copy number to cell number (Table S14 in Supplement 2). Liu et al. (2009) used 1 ml of clam tissue homogenate (equivalent to 100 mg of clam tissue), whereas this assay only used 200 µl (equivalent to 20 mg of clam tissue). The reduction of the amount of clam tissue homogenate used in the DNA extraction kit appears to have improved the recovery of QPX (Table S12 in Supplement 2), as well as reduced PCR inhibition (Tables S9 & S10 in Supplement 2). The old assay uses an estimation of 181 copies $cell^{-1}$, whereas this assay uses an estimate of 440 copies mononucleate $cell^{-1}$ (Table S14 in Supplement 2). The copy number conversion presented here is considered a better estimate because the DNA content per nucleus of 55.96 fg ± 2.95 SD equates to a genome of approximately 55 Mbp, which is more likely to reflect the size of a single genome than the Liu et al. (2009) value of 251 Mbp per cell with each cell probably containing several nuclei. The partial QPX genome assembly currently available is 34.7 Mbp and likely an underestimate (Garcia-Vedrenne et al. 2013). Recently, a complete assembly of the QPX genome revealed a genome size of 42.27 Mbp (B. Allam unpubl.), suggesting that our estimate of DNA content and QPX copies may still be an overestimation. Using the new QPX genome assembly, the DNA content would be 43.22 fg mononucleate $cell^{-1}$ with 340 ± 24.7 SD QPX copies mononucleate $cell^{-1}$. Given the uncertainties of both methods, it is likely that the QPX copy number lies between these estimations (340–440 copies mononucleate $cell^{-1}$). The method used to determine DNA content per nucleus for QPX was repeated on 2 other thraustochytrid strains that have genome assemblies, *Schizochytrium aggregatum* ATCC 28209 (40.85 Mbp) and *Aurantiochytrium limacinum* ATCC MYA-1381 (60.93 Mbp) (both available in JGI Genome Portal, https://genome.jgi.doe.gov/portal/). For *A. limacinum*, the method resulted in an average genome size of 67.86 Mbp ± 16.37 SD using 6 replicates and for *S. aggregatum*, an average size of 43.49 Mbp ± 6.26 SD using 4 replicates. The size of the assembled genomes from JGI are within the uncertainty of the values obtained using this method (within 1SD), providing strong validation for this method and the QPX copy number conversion.

Our determination of DNA content per mononucleate cell suggests that the cells used to determine the original DNA content per cell by Liu et al. (2009) contained approximately 5 nuclei. Therefore, the copy number per cell estimate by Liu et al. (2009) should be ~5 times greater than our estimate, not ~2.5 times lower. This represents an approximately 10-fold difference in copy number estimates, which we attribute to suboptimal PCR efficiency and PCR inhibition of QPX gDNA in the original assay. Using our data, we examined the effect of PCR efficiency on copy number estimate. At an efficiency of 82%, which was the efficiency of the old assay's standard curve (Liu et al. 2009), the copy number estimate is 270 copies mononucleate $cell^{-1}$. Assuming that the difference between the standard curve efficiency and QPX gDNA efficiency was similar to our assay (3% lower), we applied an efficiency of 79% to the copy number determination, which resulted in 164 copies mononucleate $cell^{-1}$, clearly illustrating the effect of PCR efficiency and inhibition on absolute quantification.

The calculation of QPX concentration by Liu et al. (2009) included PCR inhibition and QPX DNA recovery correction factors. In Liu et al. (2009), approximately 24% of clam tissue template DNA samples had to be diluted because PCR inhibition was greater than 50%. Additionally, the inhibition of samples that did not need to be diluted (inhibition < 50%) was greater than 10%, averaging 13.4% ± 20 SD. In the new assay, inhibition measured using sample template dilutions instead of an 'alien' spike (as recommended by the MIQE guidelines; Bustin et al. 2009) was minimal and not significantly different by sampling month, site or qPCR result (Tables S9–S11 in Supplement 2), suggesting that the sample matrix is similar enough to the purified standards to be used for quantification (Irwin et al. 2012). It is likely that reducing the starting volume of clam tissue and using 2 elution steps in the DNA extraction procedure reduced the impact of inhibitors simply by dilution. Therefore, we removed the PCR inhibition correction factor from our determination of QPX concentration by qPCR. The reduction of the mass of tissue used in the DNA extraction kit is likely also responsible for the nearly doubled recovery rate of QPX DNA (Table S12 in Supplement 2), compared to Liu et al. (2009) of 16.3% ± 12.3 (Table S14 in Supplement 2). We were not able to detect a pattern in the variation of recovery rate during this study, and it is possible that there was kit-to-kit variation, as Liu et al. (2009) found. Additionally, some of the improvements in both QPX recovery and PCR inhibition are likely due to proprietary changes made to the DNA

extraction kit over the years. Although the recovery rate is still low (~30%), we decided to omit it from our calculation of QPX concentration, keeping our estimates conservative, as a correction factor would only serve to inflate the quantification of gene copies and cell number.

The clams surveyed with the new assay in 2015 showed QPX prevalence that was higher and intensity (concentrations) that were lower than those obtained in previous studies at one of the same study sites (Raritan Bay) with the original assay (Liu et al. 2009, 2017, Dahl & Allam 2015). In this study, the prevalence of QPX positive–quantifiable samples ranged from 6.25 to 50% (Fig. 3) with an average value of 22% ± 17 SD, compared to the range reported by Liu et al. (2017) of 3.3 to 40% and by Dahl & Allam (2015) of 0 to 16.7%. However, the addition of the BLD samples (positive, unquantifiable) in the new assay increases total QPX prevalence, on average by 100% (Fig. 3). In terms of intensity, the highest QPX concentration measured at Raritan Bay in this study was 20.1 QPX cells mg^{-1} tissue, while Liu et al. (2009, 2017) had samples with concentrations greater than 1000 QPX cells mg^{-1} tissue. The Dahl & Allam (2015) study was more comparable to this study, with average concentrations for positive clam samples ranging from 0.59 to 28.04 QPX cells mg^{-1} tissue. Besides differences in the calculation of QPX concentration between the assays, there are other factors that could account for the differences in reported intensity. Firstly, the old assay likely overestimates concentration due to the use of circular plasmid for the standard curve (as previously discussed) as well as PCR inhibition and DNA recovery correction factors. To test this assumption, we compared a subset of the Raritan Bay samples (n = 22) from this study in both versions of the assay using the available reagents for the original version (unsupplemented Takyon master mix and circular plasmid), the Eppendorf thermocycler, inhibition assessed by spiking in 500 copies of plasmid, and use of the inhibition correction factor. Comparison of the 2 assays (Fig. 4) revealed that the old assay estimated QPX concentration as higher, on average by 115.6 times ± 331.6 SD. Secondly, the differences in QPX concentration from past studies (2006 and 2009) and this study (2015) could simply represent natural inter-annual variability in QPX intensity between the years samples were collected. While the absolute prevalence and intensity values may differ, both assays show general patterns of QPX prevalence and intensity in Raritan Bay clams that are similar (Liu et al. 2009, 2017, Dahl & Allam 2015). In general, there is higher QPX prevalence and intensity in clams in the early summer, which decreases through the fall. In this study, a similar pattern was found at Birch Creek and Peconic Estuary, while Oyster Bay, Moriches Bay and Babylon Bay showed differing trends (Fig. 3A).

The qPCR assay has already been demonstrated to detect QPX in more clams than does traditional histopathology (Liu et al. 2009). The likely explanation for this is in the focal nature of QPX disease: rather than QPX being distributed throughout the tissue, QPX lesions are generally small and confined (except in very severe cases). The qPCR assay begins with a large amount of tissue to maximize the chances of detecting a signal from a focal infection that might be missed in a small tissue sample (including that taken for histology which represents only about a $1/10\,000^{th}$ subsample of an adult clam assuming a 6 µm thick histology section from a 6 cm in length clam). The focal nature of QPX disease makes it both important and challenging to assess the value of the qPCR assay, as it alone cannot confirm active infection or pathogen viability (Burge et al. 2016, Groner et al. 2016), even though one can speculate that samples with low C_q values (high QPX copy number) likely represent genuine infections. Finding QPX-positive clams by histopathology in Raritan Bay is consistent with that area having active QPX disease and being an enzootic QPX disease location. In contrast, none of the 19 clams examined from the other sampling sites were positive by histopathology, despite several from the Peconic Estuary and Birch Creek having QPX qPCR intensities similar to clams from Raritan Bay (Fig. 3). Although Peconic Estuary and Birch Creek also had similar seasonal trends in QPX prevalence and intensity by qPCR, this suggests that there may not be active QPX disease at sites other than Raritan Bay; however, additional histopathology should be performed to test this idea, especially since QPX disease has been previously identified by histopathology in clams from Oyster Bay and Birch Creek. As expected, all BLD and negative samples were negative by histopathology, validating the qPCR assay as a screening tool to identify potentially histologically positive clams. We recommend that at a minimum, all QPX qPCR positive, quantifiable samples be examined by histopathology to confirm active infection and staging.

While we have made the argument that the new version of the assay is a better diagnostic tool, we further validated that claim by performing a regression analysis on QPX concentration (copies mg^{-1} tissue) determined by qPCR against categorical rankings of

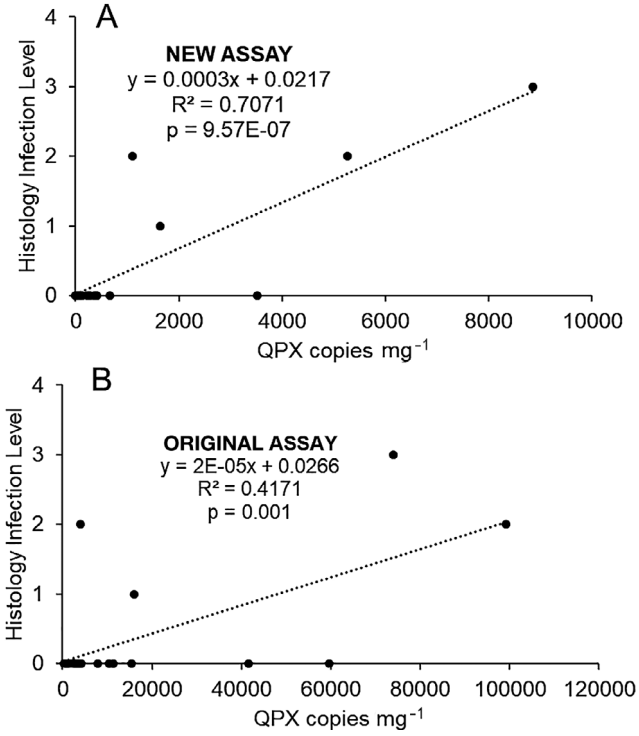

Fig. 5. Regression of QPX concentration (copies mg^{-1} tissue) determined by quantitative PCR (qPCR) against categorical ranking of QPX infection by histology (0 = none, 1 = rare, 2 = light, 3 = moderate, 4 = heavy) on the same biological samples (n = 22) from the (A) new qPCR assay and (B) old qPCR assay, illustrating a better relationship with histology using the new assay

QPX infection by histology on the subset of Raritan Bay samples (n = 22) that were processed using both versions of the assay (Fig. 5). The new, improved version of the QPX qPCR assay had a better (R^2 = 0.707) and higher probability of a statistically significant ($p = 9.57 \times 10^{-7}$) linear relationship with histology, validating that it is a better diagnostic tool compared to the original version of the assay by Liu et al. (2009).

5. CONCLUSIONS

In conclusion, we have not only provided an improved version of the QPX qPCR assay for hard clam tissue that is now in compliance with the MIQE guidelines (Bustin et al. 2009) and current common practices but is also an easy model (Fig. 1) to follow for re-optimizing, improving, changing (e.g. master mix, thermocycler, etc.), or even developing new qPCR assays. It is important to test every aspect of a new or modified assay, from the most easily characterized (i.e. primer design, cycling parameters, and specificity) to the most challenging to characterize and optimize (i.e. setup design, amplification efficiency, inhibition, and contamination). We also provide a detailed methods protocol (Supplement 3) for experimental transparency and quality control. Additionally, we provide a modified version of the MIQE checklist (Supplement 4 includes a description and blank version) that we recommend should accompany every qPCR assay that is published to be sure that all relevant experimental details are included for future users. The modified MIQE checklist for the new, improved QPX qPCR assay is presented in Table 1 as an example, with additional examples and descriptions provided in Supplement 1 of other published qPCR diagnostic assays, which clearly illustrate the lack of reporting and experimental transparency. We demonstrate the importance of assay re-assessment and validation for pathogen detection by re-optimizing an assay that was established well over a decade ago, not only making it MIQE-compliant, but also faster, cheaper, and more reliable without losing sensitivity or specificity. With up to date and diagnostically validated pathogen assays, we have the tools needed to gather more knowledge about pathogen biology and ecology, so that we can more effectively protect and manage our ecologically and socioeconomically valuable marine resources.

Acknowledgements. This research resulted from projects R/FBM-36 and R/XG-32 funded by the National Sea Grant College Program of NOAA to the Research Foundation of State University of New York on behalf of New York Sea Grant. We thank the New York State Department of Environmental Conservation (NYSDEC), specifically Dr. Soren Dahl and Captain Todd Smith, for field support and members of the Marine Animal Disease Laboratory (MADL) at Stony Brook University for assistance with sample processing.

LITERATURE CITED

Burge CA, Strenge RE, Friedman CS (2011) Detection of the oyster herpesvirus in commercial bivalve in northern California, USA: conventional and quantitative PCR. Dis Aquat Org 94:107–116

Burge CA, Kim CJ, Lyles JM, Harvell CD (2013) Special issue oceans and humans health: the ecology of marine opportunists. Microb Ecol 65:869–879

Burge CA, Mark Eakin C, Friedman CS, Froelich B and others (2014) Climate change influences on marine infectious diseases: implications for management and society. Annu Rev Mar Sci 6:249–277

Burge CA, Friedman CS, Getchell R, House M and others (2016) Complementary approaches to diagnosing marine diseases: a union of the modern and the classic. Philos Trans R Soc Lond B Biol Sci 371:20150207

Bustin SA, Benes V, Garson JA, Hellemans J and others (2009) The MIQE guidelines: minimum information for publication of quantitative real-time PCR experiments. Clin Chem 55:611–622

Bustin SA, Beaulieu JF, Huggett J, Jaggi R and others (2010) MIQE précis: practical implementation of minimum standard guidelines for fluorescence-based quantitative real-time PCR experiments. BMC Mol Biol 11: 74

Carnegie RB, Arzul I, Bushek D (2016) Managing marine mollusc diseases in the context of regional and international commerce: policy issues and emerging concerns. Philos Trans R Soc Lond B Biol Sci 371:20150215

Collier JL, Geraci-Yee S, Lilje O, Gleason FH (2017) Possible impacts of zoosporic parasites in diseases of commercially important marine mollusc species: Part II. Labyrinthulomycota. Bot Mar 60:409–417

Dahl SF, Allam B (2015) Hard clam relocation as a potential strategy for QPX disease mitigation within an enzootic estuary. Aquacult Res 47:3445–3454

Dhanasekaran S, Doherty TM, Kenneth J, Group TBTS (2010) Comparison of different standard for real-time PCR-based absolute quantification. J Immunol Methods 354:34–39

Faveri JD, Smolowitz R, Roberts SB (2009) Development and validation of a real-time quantitative PCR assay for the detection and quantification of *Perkinsus marinu*s in the eastern oyster, *Crassostrea virginica.* J Shellfish Res 28: 459–464

Ford SE, Kraeuter JN, Robert DB, Mathis G (2002) Aquaculture-associated factors in QPX disease of hard clams: density and seed source. Aquaculture 208:23–28

Gaillard C, Strauss F (1998) Avoiding adsorption of DNA to polypropylene tubes and denaturation of short DNA fragments. Tech Tips Online 3:63–65

Galluzzi L, Penna A, Bertozzini E, Vila M, Garces E, Magnani M (2004) Development of a real-time PCR assay for rapid detection and quantification of *Alexandrium minutum* (a dinoflagellate). Appl Environ Microbiol 70: 1199–1206

Garcia-Vedrenne AE, Groner M, Page-Karjian A, Siegmund GF, Singhal S, Sziklay J, Roberts S (2013) Development of genomic resources for a thraustochytrid pathogen and investigation of temperature influences on gene expression. PLOS ONE 8:e74196

Gauthier JD, Miller CR, Wilbur AE (2006) Taqman MGB real-time PCR approach to quantification of *Perkinsus marinus* and *Perkinsus* spp. in oysters. J Shellfish Res 25: 619–624

Geraci-Yee S (2021) Taking the 'X' out of QPX disease: distribution and dynamics of the hard clam pathogen, *Mucochytrium quahogii* (formerly QPX = Quahog Parasite Unknown). PhD thesis, Stony Brook University, Stony Brook, NY

Geraci-Yee S, Brianik CJ, Rubin E, Collier JL, Allam B (2021) Erection of a new genus and species for the pathogen of hard clams 'Quahog Parasite Unknown' (QPX): *Mucochytrium quahogii* gen. nov., sp. nov. Protist 172: 125793

Groner ML, Maynard J, Breyta R, Carnegie RB and others (2016) Managing marine disease emergencies in an era of rapid change. Philos Trans R Soc Lond B Biol Sci 371: 20150364

Harvell D, Aronson R, Baron N, Connell J and others (2004) The rising tide of ocean diseases: unsolved problems and research priorities. Frontiers Ecol Environ 2:375–382

Hou Y, Zhang H, Mirand L, Lin S (2010) Serious overestimation in quantitative PCR by circular (supercoiled) plasmid standard: microalgal *pcna* as the model gene. PLOS ONE 5:e9545

Howard DW, Lewis EJ, Keller BJ, Smith CS (2004) Histological techniques for marine bivalve mollusks and crustaceans, 2nd edn. NOAA Tech Memo NOS NCCOS 5. http://hdl.handle.net/1834/30812

Irwin PL, Nguyen LH, Chen CY, Uhlich GA, Paoli GC (2012) A method for correcting standard-based real-time PCR DNA quantitation when the standard's polymerase reaction efficiency is significantly different from that of the unknown's. Anal Bioanal Chem 402: 2713–2725

Johnson G, Nolan T, Bustin SA (2013) Real-time quantitative PCR, pathogen detection and MIQE. In: Wilks M (ed) PCR detection of microbial pathogens, 2nd edn. Humana Press, Totowa, NJ, p 1–16

Kleinschuster SJ, Smolowitz R, Parent J (1998) *In vitro* life cycle and propagation of Quahog Parasite Unknown. J Shellfish Res 17:75–78

Kubista M (2010) TATAA interplate calibrator SYBR protocol. User manual tataabiocenter. Tataabiocenter https://manualzz.com/doc/7008669/tataa-interplate-calibrator-user-manual

Lafferty KD, Porter JW, Ford SE (2004) Are diseases increasing in the ocean? Annu Rev Ecol Evol Syst 35:31–54

Lin CH, Chen YC, Pan TM (2011) Quantification bias caused by plasmid DNA conformation in quantitative real-time PCR assay. PLOS ONE 6:e29101

Liu Q, Allam B, Collier JL (2009) Quantitative real-time PCR assay for QPX (Thraustochytriidae), a parasite of the hard clam (*Mercenaria mercenaria*). Appl Environ Microbiol 75:4913–4918

Liu Q, Collier JL, Allam B (2017) Seasonality of QPX disease in the Raritan Bay (NY) wild hard clam (*Mercenaria mercenaria*) population. Aquacult Res 48:1269–1278

Lyons MM, Smolowitz R, Dungan CF, Roberts S (2006) Development of a real time quantitative PCR assay for the hard clam pathogen Quahog Parasite Unknown (QPX). Dis Aquat Org 72:45–52

Markowitz KN, Williams JD, Krause MK (2016) Development of quantitative PCR assay for detection of the trematode parasite *Proctoeces maculatus* in the blue mussel *Mytilus edulis*. Dis Aquat Org 122:125–136

McCallum H, Kuris A, Harvell C, Lafferty K, Smith G, Porter J (2004) Does terrestrial epidemiology apply to marine systems? Trends Ecol Evol 19:585–591

Polinski M, Lowe G, Meyer G, Corbeil S, Colling A, Caraguel C, Abbott CL (2015) Molecular detection of *Mikrocytos mackini* in Pacific oysters using quantitative PCR. Mol Biochem Parasitol 200:19–24

Qian H, Liu Q, Allam B, Collier JL (2007) Molecular genetic variation within and among isolates of QPX (Thraustochytridae), a parasite of the hard clam *Mercenaria mercenaria.* Dis Aquat Org 77:159–168

Ramilo A, Navas JI, Villalba A, Abollo E (2013) Species-specific diagnostic assays for *Bonamia ostreae* and *B. exitiosa* in European flat oyster *Ostrea edulis*: conventional, real-time and multiplex PCR. Dis Aquat Org 104: 149–161

Renault TC (2008) Genomics and mollusc pathogens: trends and perspective. J Vet Clin Sci 1:4–14

Ríos R, Aranguren R, Gastaldelli M, Arcangeli G, Novoa B, Figueras A (2020) Development and validation of a specific real-time PCR assay for the detection of the parasite *Perkinsus olseni*. J Invertebr Pathol 169: 107301

RStudioTeam (2018) RStudio: integrated develpoment for R. RStudio, Boston, MA

Svec D, Tichopad A, Novosadova V, Pfaffl MW, Kubista M (2015) How good is a PCR efficiency estimate: recommendations for precis and robust qPCR efficiency assessments. Biomol Detect Quantif 3:9–16

Ulrich PN, Ewart JW, Marsh AG (2007) Prevalence of *Perkinsus marinus* (dermo), *Haplosporidium nelsoni* (MSX), and QPX in bivalves of Delaware's inland bays and quantitative, high-throughput diagnosis of dermo by QPCR. J Eukaryot Microbiol 54:520–526

Ward JR, Lafferty KD (2004) The elusive baseline of marine disease: Are diseases in ocean ecosystems increasing? PLOS BIOL 2:e120

Wickham H (2016) ggplot2: elegant graphics for data analysis. Springer-Verlag, New York, NY

Wilbur AE, Ford SE, Gauthier JD, Gomez-Chiarri M (2012) Quantitative PCR assay to determine prevalence and intensity of MSX (*Haplosporidium nelsoni*) in North Carolina and Rhode Island oysters *Crassostrea virginica.* Dis Aquat Org 102:107–118

Editorial responsibility: Kimberly Reece, Gloucester Point, Virginia, USA
Reviewed by: C. Audemard and 1 anonymous referee

Submitted: March 26, 2021
Accepted: December 17, 2021
Proofs received from author(s): March 21, 2022